Synthesis and Characterization of Protonated Zirconium Trisilicate and Its Exchange Phases with Strontium

Christopher S. Fewox and Abraham Clearfield*

Texas A & M University, Department of Chemistry, P.O. Box 30012, College Station, Texas 77842-3012

Received: November 1, 2007; In Final Form: December 27, 2007

A partially protonated form of the mineral umbite has been prepared by ion exchange of $K_2ZrSi_3O_9 \cdot H_2O$ with acetic acid. The protonated phase, compound **1,** is assigned the formula $H_{1.45}K_{0.55}ZrSi_3O_9 \cdot 2H_2O$ and crystallizes in the space group $P2_1/c$ with unit cell dimensions of $a = 7.1002(2)$, $b = 10.1163(3)$, $c = 13.1742(5)$, and $\beta = 91.181(1)°$. The characteristic building blocks of the acid phase are almost identical to those of the parent compound. The framework is composed of polymeric chains of trisilicate groups linked by zirconium atoms, resulting in zeolite-type channels. When viewed down the *a* axis, two unique ion-exchange channels can be seen. Site 1 is marked by a 12-membered ring and contains 2 cations. Site 2, a 16-membered ring, contains 4 water molecules. Compound **2**, consists of a mixed Sr^{2+} and K^+ phase synthesized from **1** by ion exchange with $Sr(NO_3)_2$. Compound **2** has the formula $K_{0.34}Sr_{0.83}ZrSi_3O_9 \cdot 1.8H_2O$ and crystallizes in the same space group $P2_1/c$. It has cell dimensions of $a = 7.1386(3)$, $b = 10.2304(4)$, $c = 13.1522(4)$, and $\beta = 90.222(1)°$. The Sr^{2+} cations are distributed evenly among the two exchange sites, showing no preference for either cavity. Compound **3** is the fully substituted Sr phase, $SrZrSi_3O_9 \cdot 2H_2O$, and retains the same space group as that of the previous two compounds having unit cell dimensions of $a = 7.1425(5)$, $b = 10.2108(8)$, $c = 13.0693(6)$, and $\beta = 90.283(1)°$. The strontium cations show a slight affinity for ion-exchange site 2, having a higher occupancy of 0.535, while site 1 is occupied by the remainder of the Sr^{2+} cations with an occupancy of 0.465. Batch uptake studies demonstrate a selectivity series among alkaline earth cations of $Ba^{2+} > Sr^{2+} > Ca^{2+} > Mg^{2+}$.

Introduction

For many years, the buildup of nuclear waste from power plants and weapons facilities has been a pressing problem for the environment. Disposal strategies have relied on the separation of ^{137}Cs and ^{90}Sr from their constituents in waste streams. These elements are required to be segregated because of their high heat generation stemming from radioactive decay, their environmental threat, and the long half-lives of these elements. Separation of these isotopes also has the effect of reducing the volume of waste after vitrification, a process that solidifies the waste for permanent disposal, typically in borosilicate or phosphate glass. This allows for increased storage space and reduces the need for future disposal facilities. With half-lives of approximately 30 years, separated strontium and cesium waste can be decommissioned and disposed of safely in 10 half-lives or 300 years.[1]

Research on ion exchangers to facilitate separations in nuclear waste streams has been a subject of research for many years. In order to be considered a serious candidate for radioactive waste remediation, an ion exchanger must have the following attributes. (i) The ion exchanger must be thermally stable and be able to withstand intense ionizing radiation.[2] (ii) Chemical stability is required due to extreme pH which extends to alkaline and acidic media. (iii) The exchanger must exhibit high selectivity in competing media, where concentrations of Na^+ can be greater than 6 M.

Solvent extraction using complexing agents such as crown ethers and calixarenes have been tested; however, their resistance to ionizing radiation is suspect.[3,4] Natural clays, micas, and zeolites like clinoptilolite have been shown to possess ion-exchange capabilities and can be highly selective and thermally stable but can deteriorate due to dissolution of silicon and aluminum in highly alkaline or acidic solutions.[5−7] Crystalline antimonic acids, microporous tungstates, and mixed metal antimonates have also received attention for their ion-exchange capabilities and potential uses in waste remediation.[8−12] Other titanates such as monosodium titanate and sodium nonatitanate display an exceptional ability to sorb strontium, as well as actinides; however, these materials are poorly crystalline, and ergo, their structures and mechanism of ion exchange have been difficult to elucidate.

In the past decade, attention has been turned to new classes of inorganic ion exchangers. Open-framework compounds with zeolite-type pores have shown high thermal stability and high selectivity in competitive media.[13] Titanium silicates with tunnel-type structures have been tested in waste simulants and have shown a considerable ability to sequester cesium and strontium.[14−16] The crystal structures of these silicotitanates have been solved and have shown that their selectivity for cesium can be attributed to stronger coordination to the framework and interstitial water.

Another group of metal silicates has been examined for their ability to selectively acquire cesium. Silicates with the topology of the mineral umbite provide an excellent system for the study of the origins of ion-exchange selectivity.[17−19] Phases interchanging the octahedral metal connecting the polysilicate chains have been synthesized. Titanium and tin forms of the trisilicate show different affinities for different alkali cations.[20,21] The difference in uptake is attributed to the change in pore size as a smaller or larger chain-linking metal is used. By crystallizing in the space group $P2_12_12_1$, the unit cell volume of these materials expands by 100 $Å^3$ when going from the potassium

* To whom correspondence should be addressed. Tel.: +1 979 845 2936. Fax: +1 979 845 2370. E-mail: Clearfield@mail.chem.tamu.edu.

10.1021/jp709592x CCC: $40.75
Published on Web 02/29/2008

titanium phase to the germanium-substituted potassium zirconium phase synthesized by Yaghi and co-workers.[22] A mixed K^+/Na^+ phase has been synthesized by Lui and Thomas, which crystallizes in the monoclinic space group $P2_1/c$ rather than in the orthorhombic one.[23] Phase transformations between the orthorhombic and monoclinic also occur during ion exchange; however, this is not entirely understood. Other monoclinic phases are seen in other forms of the trisilicate, including the partially protonated titanium phase and the lead-containing kostylevite phase, which does not show ion-exchange properties.[21]

In order to better understand the mechanism of ion exchange in 3D tunnel framework compounds, the partially protonated phase of $K_2ZrSi_3O_9 \cdot H_2O$ has been prepared. It is hoped that this system will serve as a model for ion-exchange processes in inorganic framework ion exchangers. A complete series of group I zirconium trisilicate ion-exchange compounds has already been synthesized and characterized.[24,25] We report here the protonated phase of zirconium trisilicate and a new study on its exchange phases with group II cations.

Experimental Section

Reagents. All reagents were of analytical grade purity (Aldrich) and were used without further purification. ^{90}Sr was procured from Perkin-Elmer.

Analytical Procedures and Instrumentation. Phase identification and structural data sets were collected using a Bruker-AXS D8 VARIO powder diffractometer. Thermal gravimetric analysis was conducted on a TA Instruments TGA Q 500 unit. A constant temperature ramp of 5 °C/min was applied while the sample was under a 9:1 nitrogen to air volume ratio. Potassium and strontium analysis was performed on a Varian AA 250 atomic absorption spectrometer under an acetylene nitrous oxide flame. Samples for AA analysis were prepared by digestion of the solid in hydrofluoric acid. Measurements of ^{90}Sr uptake were performed on a Wallac 1410 liquid scintillation counter. Titrations and pH measurements were conducted on a TitraLab TIM860 titration manager. SEM images were taken on a Zeiss 1530VP FE-SEM.

Synthesis and Ion Exchange. Potassium zirconium trisilicate, $K_2ZrSi_3O_9 \cdot H_2O$, was synthesized hydrothermally by modification of methods previously reported by Poojary et al.[20] An amount of 7.0 grams of silicic acid was dissolved in 45 mL of 4 M KOH and 10 mL of isopropanol. A volume of 13.5 mL of a 70% solution of zirconium isopropoxide in isopropanol was diluted with 10 mL of isopropanol and added dropwise to the previous solution. The mixture was divided in two and placed in 100 mL Teflon-lined autoclaves. The reaction was carried out at 180 °C. After 5 days, a white precipitate was isolated and washed with distilled water and dried at 60 °C.

Compound **1**, $H_{1.45}K_{0.55}ZrSi_3O_9 \cdot 2H_2O$, was synthesized by shaking $K_2ZrSi_3O_9 \cdot H_2O$ in 0.1 M acetic acid at a volume to mass ratio of 500:1 for 24 h at room temperature. The product was collected by vacuum filtration and washed with distilled water and acetone. The dry product was then shaken in 0.5 M acetic acid for 24 h. The product was again collected by vacuum filtration and rinsed thoroughly with water and acetone until no odor of acetic acid was detected. Anal. Calcd. for $K_{0.56}H_{1.44}ZrSi_3O_9 \cdot 2H_2O$: Zr, 24.11; Si, 22.28; K, 5.79. Found: Zr, 23.89; Si, 21.61; K, 5.71.

Compound **2**, $K_{0.34}Sr_{0.83}ZrSi_3O_9 \cdot 1.8H_2O$, was synthesized by shaking 1.0 g of **1** in 500 mL of 0.5 M $SrCl_2$ for 24 h at room temperature. The white powder was washed first with water and then acetone and dried at room temperature. Anal. Calcd. for $K_{0.34}Sr_{0.83}ZrSi_3O_9 \cdot 1.8H_2O$: Zr, 20.62; Si, 19.05; K, 3.00; Sr, 16.43. Found: Zr, 20.70; Si, 19.51; K, 3.31; Sr, 16.58.

Compound **3**, $SrZrSi_3O_9 \cdot 2H_2O$, was synthesized by ion exchange at elevated temperature. An amount of 2.0 g of **1** was placed in a 250 mL round-bottom flask along with 200 mL of 1.0 M $SrCl_2$. This mixture was stirred at 90 °C for 24 h. The mixture was allowed to settle, and the supernatant liquid was decanted and saved. A fresh 200 mL sample of 1.0 M $SrCl_2$ was added and heated again for 24 h. This process was repeated until the presence of potassium in the supernatant liquid was undetectable by AA spectroscopy. Anal. Calcd. for $SrZrSi_3O_9 \cdot 2H_2O$: Zr, 20.61; Si, 19.03; Sr, 19.80. Found: Zr, 20.76; Si, 19.61; Sr, 20.18.

X-ray Data Collection and Structure Refinement. Data sets were collected on a Bruker-AXS D8 VARIO powder diffractometer with standard vertical Bragg−Brentano geometry and a linear PSD detector. The diffractometer was equipped with a germanium monochromator, allowing the use of Cu $K\alpha_1$ radiation only with a wavelength of 1.54056 Å. Powders were loaded on a quartz disc, which was spun during data collection to reduce any scattering effects due to preferred orientation. The operating voltage and current were 40 kV and 50 mA, respectively. Data were collected at room temperature with 2θ ranging from 5 to 130 degrees. A step size of 0.016 degrees and a scan time of 15 s per step were employed.

Powder patterns were indexed using TREOR, ITO, and DICVOL methods found in the FullProf program suite.[26−28] Profile function fitting using the LeBail method and Reitveld refinement were accomplished using the GSAS program suite.[29,30] No corrections were made for absorption and neutral atom scattering factors were used as stored in GSAS. No attempt was made to model the preferred orientation.

Observed and calculated XRD profiles are displayed in Figure 1. Compound **1** crystallizes in the monoclinic space group $P2_1/c$ with cell dimensions of $a = 7.1002(2)$, $b = 10.1163(3)$, $c = 13.1742(5)$, and $\beta = 91.181(1)°$. The structure of the potassium phase and the partially substituted proton phase are very similar. However, a phase change from an orthorhombic unit cell, space group $P2_12_12_1$, for the K phase to a monoclinic cell has occurred. To use the potassium phase as a starting model in structural refinement, it was necessary to transform the original atomic coordinates by the matrix given in eq 1

$$\begin{pmatrix} x & & \\ & y & \\ & & z \end{pmatrix} \cdot \begin{pmatrix} z/x & & \\ & \left(\frac{1}{4}y + x/y\right) & \\ & & y/z \end{pmatrix} = \begin{pmatrix} z & & \\ & \left(\frac{1}{4} + x\right) & \\ & & y \end{pmatrix} \quad (1)$$

Once profile fitting was completed and the framework atomic coordinates were transformed into their new system, bond distance restraints were applied to Si−O and Zr−O contacts. The position of zirconium was refined, and subsequently, that of each individual trisilicate group was refined also. Fourier difference maps were constructed to reveal the position of the missing cations and waters. Once the positions were input, the atomic coordinates of the framework were again refined. Next, the cation and water positions were refined without moving the framework. This seesaw approach was continued until least-squares refinement converged rapidly and the shift in atomic coordinates was less than 0.1% of the starting value. The potassium site occupancy for **1** was then refined, while isotropic thermal factors were held constant. Once site occupancy was established, isotropic thermal factors for zirconium, potassium, and water oxygens were refined. An attempt to assign hydrogen positions was made, however the result did not make chemical sense, and these atoms were not included in the final refinement.

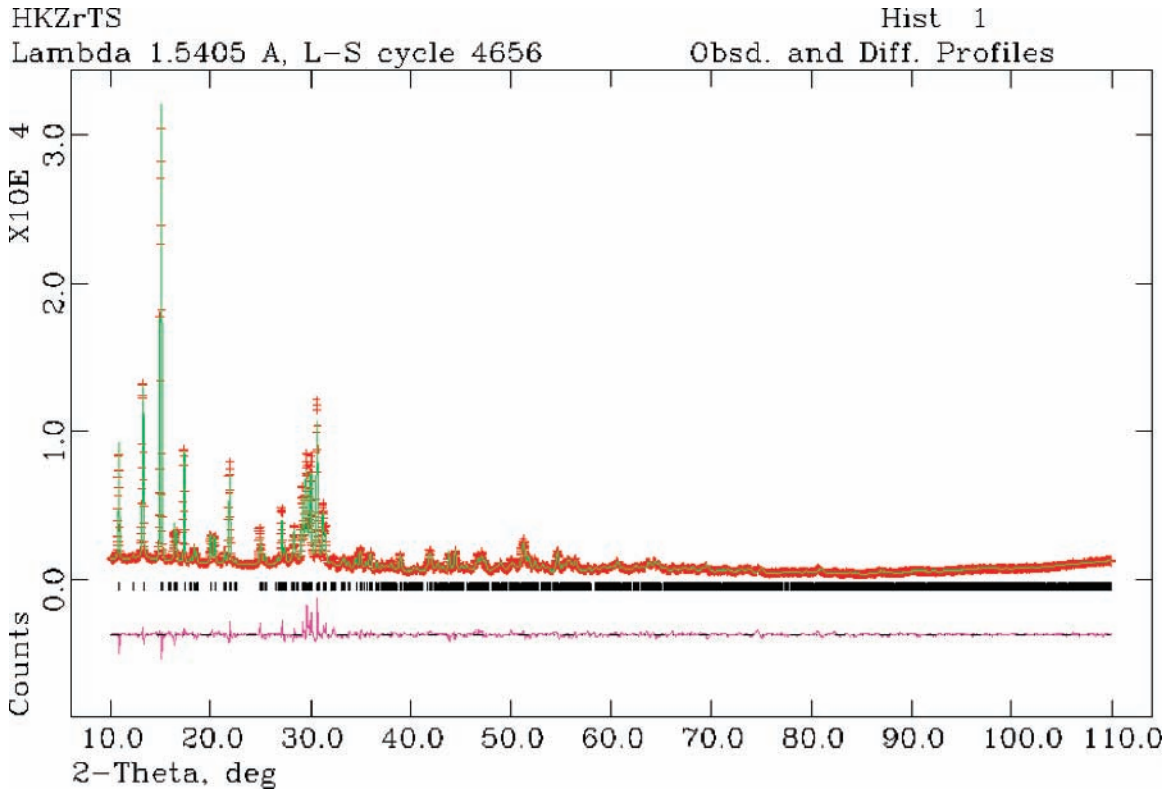

Figure 1. Observed (+) and calculated (−) profiles for final Reitveld refinement of **1**. A difference plot is shown in the bottom as the pink line. Reflections are marked by the black bars.

Selectivity and Ion-Exchange Kinetics. The rate of strontium uptake was measured under infinite solution volume conditions as specified by Helfferich.[31] Vigorous stirring was employed to ensure particle-diffusion-controlled kinetics. The rate of Sr^{2+} uptake was measured by tracing a 1.0 equiv $SrCl_2$ solution with enough ^{90}Sr to yield a count rate of ~60 000 counts per minute. An amount of 0.2 grams of ion exchanger was added to 100 mL of this solution under vigorous stirring, and 1.0 mL aliquots were taken at designated times and filtered through a Millipore 0.22 μm syringe filter tip. The solution was then shaken with 18 mL of scintillation cocktail, and the amount of ^{90}Sr was measured by liquid scintillation counting on a Wallac 1410 liquid scintillation counter.

Mass diffusion coefficients for group II metals were measured using TitraLab TIM860 titration manager. To 50 mL of water, adjusted to a pH of 7.0, was added 0.10 grams of **1**. Particles were sieved before addition to achieve an average size of 150 μm. Once an equilibrium pH was achieved, a 62 μL spike containing 1.0 equiv of M^{2+} was added, and the change in pH over time was recorded.

The ion-exchange selectivity series for alkaline earth metals was determined by shaking 0.1 g of **1** and 1.0 equiv of $M(NO_3)_2$ in 50 mL of deionized water adjusted to the desired pH for 24 h. The uptake of each cation was measured by determining the concentration of K^+ and M^{2+} by atomic absorption. A suitable sample for AA was prepared by digesting approximately 5 mg of the solid exchange phase in 2 mL of concentrated HF at room temperature and diluting to 1.000 L.

Results

Structure of $H_{1.45}K_{0.55}ZrSi_3O_9 \cdot 2H_2O$ (1). Essential crystallographic data are shown in Table 1. The structure of **1** is similar to the umbite phase. Linear chains of polymeric silicate groups are linked by zirconium octahedra, forming two unique ion-exchange sites. These sites are best viewed in a ball and stick representation looking down the *a* axis (Figure 2). Upon conversion to the acid phase, the unit cell volume decreases approximately 40 Å^3, and the space group changes from $P2_12_12_1$ to $P2_1/c$. This is unusual in that the transformation from a noncentrosymmetric space group to a Laue symmetry that contains an inversion center is not often observed.

TABLE 1: Crystallographic Data for the Zirconium Trisilicate Phases[a]

	1	2	3
fw	378.81	437.87	443.08
space group	$P2_1/c$	$P2_1/c$	$P2_1/c$
a (Å)	7.1000(2)	7.1386(3)	7.1425(5)
b (Å)	10.1169(3)	10.2304(4)	10.2108(8)
c (Å)	13.1742(5)	13.1522(4)	13.0693(6)
β	91.181(1)°	90.222(1)°	90.283(1)°
V (Å^3)	946.09(5)	961.25(5)	952.20(17)
Z	4	4	4
D_{calc} (g/cm^3)	2.618	3.003	3.060
no. of reflections	1406	1247	866
R_{wp}	0.0905	0.0789	0.0710
R_p	0.0672	0.0671	0.0543

[a] Formulas: (**1**) $K_{0.56}H_{1.44}ZrSi_3O_9 \cdot 2H_2O$; (**2**) $K_{0.34}Sr_{0.83}ZrSi_3O_9 \cdot 1.8H_2O$; (**3**) $SrZrSi_3O_9 \cdot 2H_2O$.

Positional parameters for **1** are shown in Table 2, and selected framework bond distances for all compounds are shown in Table 3. Besides the change in space group, the most obvious structural difference between the parent compound, $K_2ZrSi_3O_9 \cdot H_2O$, and compound **1** is the addition of 1 mol of water. The hydrogen bonding of water in site 2 to framework oxygens was shown by Zou and Dadachov in single-crystal X-ray diffraction studies of the potassium titanium trisilicate.[32] In this case, a second water resides in site 2, which was previously occupied by K^+. Selected O−O distances between water molecules and framework oxygens, listed in Table 4, suggest the presence of

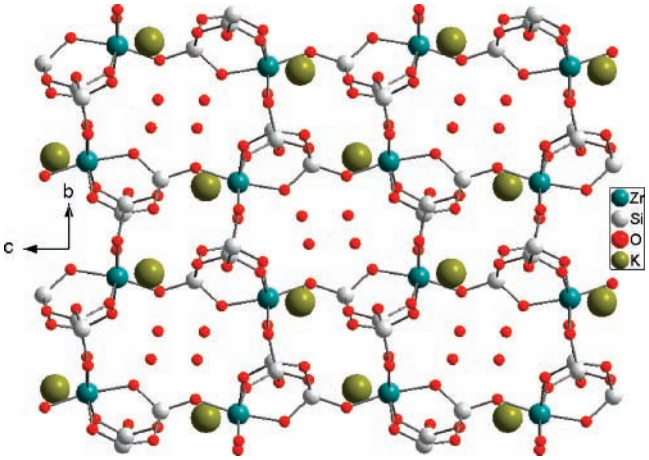

Figure 2. Exchange sites 1 in the large ring and 2 containing the K^+ ions as found in $H_{1.45}K_{0.55}ZrSi_3O_9 \cdot 2H_2O$. The view is down the *a* axis.

TABLE 2: Positional and Thermal Parameters for $K_{0.56}H_{1.44}ZrSi_3O_9 \cdot 2H_2O$

	x	y	z	U_{iso}[a]
Zr1	0.2589(6)	0.70456(28)	0.20017(26)	0.0380(5)
Si2	0.0112(8)	0.4282(5)	0.1826(4)	0.008
Si3	0.7352(9)	0.2820(5)	0.0557(4)	0.008
Si4	0.5778(8)	0.8903(6)	0.3276(4)	0.008
O5	0.2308(19)	0.6715(7)	0.3541(5)	0.004
O6	0.0390(15)	0.5871(6)	0.2025(10)	0.004
O7	0.2226(20)	0.7674(10)	0.0596(5)	0.004
O8	0.4794(13)	0.8180(8)	0.2264(6)	0.004
O9	0.0960(14)	0.8620(8)	0.2179(6)	0.004
O10	0.4325(17)	0.5491(6)	0.1996(9)	0.004
O11	0.2030(7)	0.3415(8)	0.1637(8)	0.004
O12	0.5247(9)	0.3521(9)	0.0658(5)	0.004
O13	0.878(1)	0.4091(7)	0.0804(5)	0.004
Ow1	−0.0992(24)	0.5592(24)	0.4116(12)	0.155(14)
K15[b]	0.7521(19)	0.6878(10)	0.0938(8)	0.0115(32)
Ow2	0.6344(14)	0.5617(11)	0.5648(8)	0.092(11)

[a] $U_{iso} = B_{iso}/8\pi^2$. [b] Occupancy factor = 0.55.

TABLE 3: Selected Framework Bond Distances (Å) for Compounds 1−3

bond	1	2	3
Zr1−O5	2.069(8)	2.118(7)	2.116(9)
Zr1−O6	1.963(10)	1.976(10)	2.104(13)
Zr1−O7	1.970(8)	2.075(8)	2.009(9)
Zr1−O8	1.966(10)	2.024(11)	1.977(12)
Zr1−O9	1.985(9)	2.035(10)	2.010(12)
Zr1−O10	1.998(9)	2.067(10)	2.064(13)
Si2−O6	1.640(8)	1.644(9)	1.642(10)
Si2−O9	1.67(1)	1.659(11)	1.649(12)
Si2−O11	1.643(8)	1.651(9)	1.645(9)
Si2−O13	1.641(9)	1.649(10)	1.630(11)
Si3−O5	1.646(9)	1.646(9)	1.646(10)
Si3−O7	1.613(13)	1.663(15)	1.662(17)
Si3−O12	1.662(9)	1.662(10)	1.666(11)
Si3−O13	1.665(9)	1.67(1)	1.662(11)
Si4−O8	1.662(10)	1.658(11)	1.630(12)
Si4−O10	1.647(9)	1.635(9)	1.627(11)
Si4−O11	1.635(8)	1.638(8)	1.637(10)
Si4−O12	1.641(9)	1.65(1)	1.618(11)

hydrogen bonding between waters in the cavity as most of the distances are approximately 2.8 Å.

Table 5 shows selected cation−oxygen distances of less than 3.6 Å for compounds **1**−**3**. The coordination environment of the remaining K^+ ion in site 1 is similar to that of the parent compound. Potassium cations are 10-coordinate, with an average M15−O distance of 3.105(2) Å, and have close contacts with O6 and Ow2 of 2.666(16) Å and 2.694(15), respectively. For

TABLE 4: Selected O−O Distances for Compound 1 Indicate the Presence of Hydrogen Bonding

water−oxygen pair	distance (Å)
Ow1−Ow2	2.794(21)
Ow2−Ow2′	2.825(16)
Ow1−O9	2.625(33)
Ow2−O8	2.706(14)
Ow1−Ow1′	2.951(26)

TABLE 5: Cation−Oxygen Distances

compound	M14−O	distance (Å)	M15−O	distance (Å)
(**1**) $K_{0.56}H_{1.44}Zr$-$Si_3O_9 \cdot 2H_2O$			K15−O6	2.666(16)
			K15−O7	3.474(19)
			K15−O8	2.946(15)
			K15−O9	3.407(15)
			K15−O10	3.033(16)
			K15−O11	3.560(15)
			K15−O11′	3.428(15)
			K15−O12	2.879(14)
			K15−O13	2.964(13)
			K15−Ow2	2.694(15)
(**2**) $K_{0.35}Sr_{0.825}Zr$-$Si_3O_9 \cdot H_2O$	M14−O5	2.650(12)	M15−O6	2.767(18)
	M14−O7	3.242(13)	M15−O8	3.049(16)
	M14−O7′	3.204(19)	M15−O9	3.417(16)
	M14−O9	2.950(12)	M15−O10	2.841(18)
	M14−Ow1	2.701(18)	M15−O11	3.577(12)
	M14−Ow1′	3.492(20)	M15−O11′	3.408(12)
			M15−O12	3.090(15)
			M15−O13	3.190(12)
			M15−O13′	3.246(16)
(**3**) $SrZrSi_3O_9 \cdot H_2O$	Sr14−O5	2.607(16)	Sr15−O6	2.799(30)
	Sr14−O6	3.383(19)	Sr15−O8	3.026(26)
	Sr14−O7	3.176(22)	Sr15−O9	3.286(24)
	Sr14−O9	2.667(17)	Sr15−O10	2.579(27)
	Sr14−Ow1	2.896(18)	Sr15−O12	3.187(23)
			Sr15−O13	3.311(25)
			Sr15−O13¢	3.278(20x

the 10-coordinate potassium ion, the sum of ionic radii between K^+ and O^{2-} water oxygen can be considered to be approximately 2.94 Å.[33] There are four additional contacts (M15−O8, M15−O10, M15−O12, and M15−O13) within 0.2 Å of this value, hinting that the potassium in this channel is still held tightly.

Structure of $K_{0.34}Sr_{0.83}ZrSi_3O_9 \cdot 1.8H_2O$ (2). The incorporation of Sr^{2+} has some interesting consequences; however, the space group of the protonic phase and the basic structure of the zirconium trisilicate is conserved. The unit cell increases only slightly, ∼15 Å^3, to allow for the exchange of the larger strontium cation for the proton. Analysis of site occupancy shows that Sr^{2+} is almost evenly distributed among sites 1 and 2, 0.42 and 0.41, respectively. Structural refinement of cation occupancy also shows movement of the K^+, which formerly occupied only exchange site 1, into site 2. K^+ occupancy factors for sites 1 and 2 are 0.20 and 0.14, respectively. The arrangement of the water molecules has shifted within the framework. Ow2 and Ow3 are found in both cation sites 1 and 2 but unevenly due to the cation distribution. Ow1 remains in its original position and is assigned an occupancy factor of 1.

The coordination spheres of the cations in sites 1 and 2 are quite different. Cations in site 1 can be said to be nine-coordinate, having an average contact distance of 3.176(15) Å, with the shortest and longest distances being M15−O6 and M15−O11 at 2.767(18) and 3.577(12) Å, respectively. Cations located in site 2 are six-coordinate and have a much shorter average contact distance of 3.04(1) Å. This is due to the closer

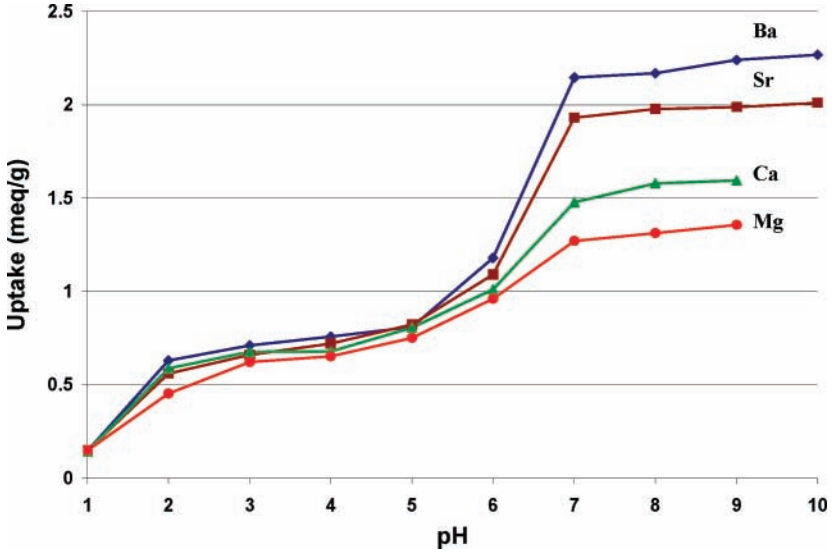

Figure 3. Room-temperature, pH-dependent uptake of alkaline earth cations in $H_{1.45}K_{0.55}ZrSi_3O_9 \cdot 2H_2O$.

TABLE 6: Mass Diffusion Coefficients for the Uptake of M^{2+} by Compound 1

cation	diffusion coefficient D ($\mu m^2 \cdot s^{-1}$)	Vermeulen regression statistics (R^2, χ^2/DoF)
Mg^{2+}	0.091	0.990, 0.00069
Ca^{2+}	0.205	0.986, 0.00077
Sr^{2+}	0.479	0.991, 0.00075
Ba^{2+}	0.183	0.987, 0.00077

contacts of M14−O5 and M14−Ow1, which are 2.650(12) and 2.701(18) Å, respectively.

Structure of $SrZrSi_3O_9 \cdot 2H_2O$ (3). The fully substituted strontium trisilicate crystallizes in the monoclinic space group $P2_1/c$. The unit cell has decreased in size by 10 $Å^3$ in comparison to compound **2**. Two moles of water are present, one in the larger cavity and the other split among the ion-exchange sites. Strontium is found in both ion-exchange sites. The occupancy factors for sites 1 and 2 are 0.535 and 0.465, respectively.

Strontium cations in site 1 are more tightly held as the ion-exchange site creates a basket or bowl shape to cradle the cation. Sr^{2+} in site 1 is seven-coordinate, with its shortest and longest contacts being Sr15−O10 and Sr15−O13′, which are 2.579(28) and 3.278(20) Å, respectively.

Strontium cations in site 2 are coordinated by only five oxygens, four oxygens from the framework and one water molecule. The Sr14−Ow1 distance is longer than the predicted, being 2.896(18) Å. The closest contact is for Sr14−O5, which is 2.607(16) Å. If we consider the ionic radius of six-coordinate Sr^{2+} as 1.18 Å, then the sum of ionic radii in a Sr−O bond should be approximately 2.6 Å. The Sr14−O9 bond length is 2.667(17) Å, and the O5−Sr14-O9 bond angle is 102.6(5)°. A bond angle of 90.3(6)° is observed for O5−Sr14−Ow1.

Selectivity and Kinetics of M^{2+} Cation Exchange and ^{90}Sr Uptake. The selectivity of alkali cations in zirconium trisilicate has been probed over the entire pH range. In acidic media, the selectivity series is $Rb^+ > Cs^+ > K^+ > Na^+ > Li^+$. In basic media, the selectivity series still favors Rb^+, with little difference in the uptake of other alkali metals.[20] The uptake of alkaline earth cations for compound **1** is shown in Figure 3. There is no selectivity for alkaline earth cations in acidic media. Beyond pH 6, however, the selectivity series is defined as $Ba^{2+} > Sr^{2+} > Ca^{2+} > Mg^{2+}$.

Mass diffusion coefficients are listed in Table 6. Values were calculated by fitting the fractional attainment of equilibrium over time, $U(t)$, to Vermeulen's approximation, eq 2

$$U(t) = \left[1 - \exp\left(\frac{D_i t \pi^2}{r_o^{\,2}}\right)\right]^{1/2} \qquad (2)$$

D_i is the mass diffusion coefficient, r_o is the average particle radius, in this case, 150 μm, and t is time.

The rate of uptake does not mimic the pattern observed in the selectivity. The absorption of Sr^{2+} by compound **1** is the fastest, with a mass diffusion coefficient of 0.479 $\mu m^2 \cdot s^{-1}$. The kinetics of uptake for Ba^{2+} and Ca^{2+} are similarly fast, having mass diffusion coefficients of 0.183 and 0.205 $\mu m^2 \cdot s^{-1}$, respectively, while Mg^{2+} shows the slowest uptake. Plots of the experimental and calculated data demonstrating their agreement are shown in Figure 4.

The kinetic data derived from radio tracer experiments with ^{90}Sr do not support the data found by measuring the change in pH over time. A separate plot of and fit of U versus time is shown in Figure 5. The mass diffusion coefficient found for the uptake of ^{90}Sr is 197.2 $\mu m^2 \cdot s^{-1}$. The reason for this disparity is twofold. First, in measuring the change in pH over time, the physical phenomenon being observed is the increase in $[H^+]$ as Sr^{2+} is exchanged in. This method does not include the direct exchange of Sr^{2+} for K^+. Another process that occurs is K^+/H^+ exchange. This process is observed simultaneously and has the effect of slowing down the shift to lower pH as the protons liberated by the influx of Sr^{2+} are taken back up and exchanged for K^+. When conducting the radio strontium experiments, the only physical observation is the disappearance of ^{90}Sr over time. In this case, the rate does not depend on the process or mechanism of uptake; it only depends on the fact that some of the strontium that was once in solution is now exchanged.

The second and unfortunately inescapable challenge in kinetic studies in this system is the fact that the starting and final phases are not pure, that is, they contain many different cations, such as K^+, Sr^{2+}, H^+, and so forth. The reaction is not a simple complete A-for-B exchange. This contributes to the complications when attempting to describe the mechanism of exchange also and requires equations with fewer and less descriptive parameters to be utilized.

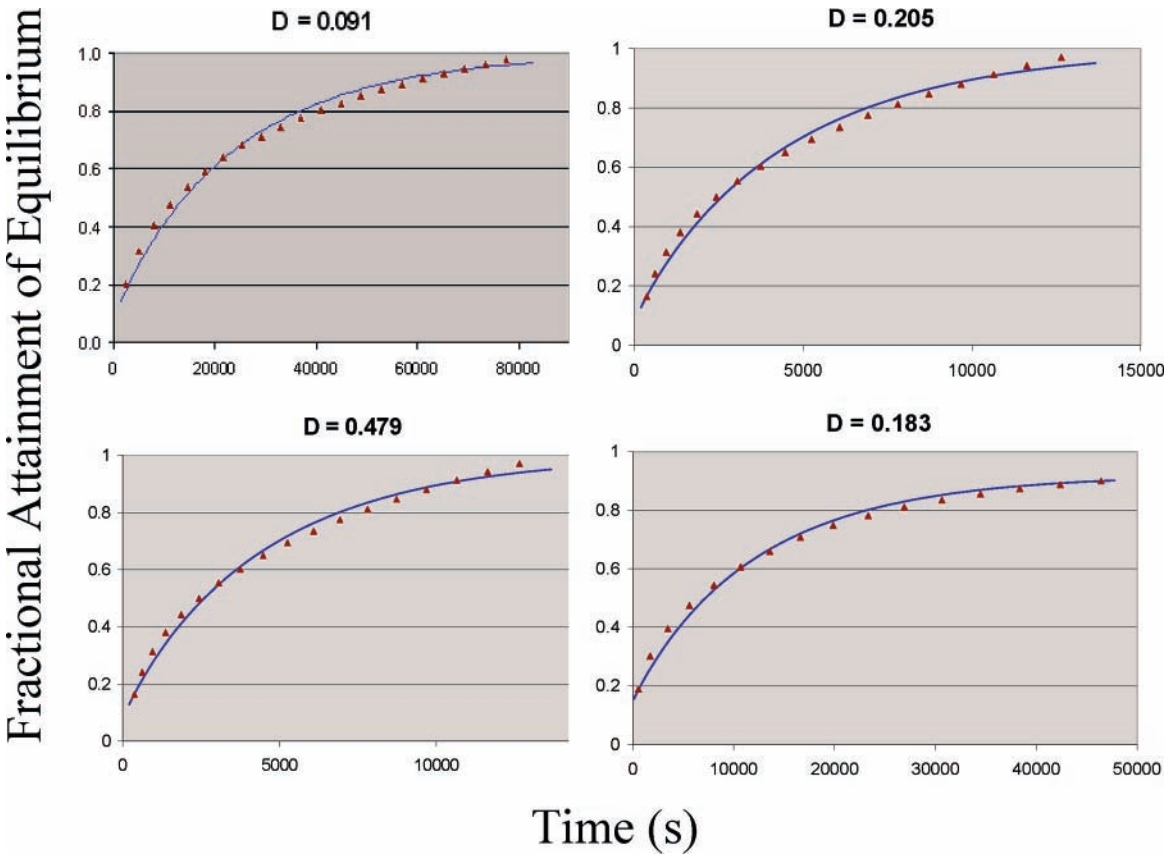

Figure 4. Kinetic data for the uptake of alkaline earth metals in $H_{1.45}K_{0.55}ZrSi_3O_9 \cdot 2H_2O$ at neutral pH. Plots fitting Vermeulen's approximation to observed changes in fractional attainment of equilibrium over time. Triangles represent observed data, and the solid line represents the Vermeulen model. Mass diffusion coefficients are in units of $\mu m^2 \cdot s^{-1}$.

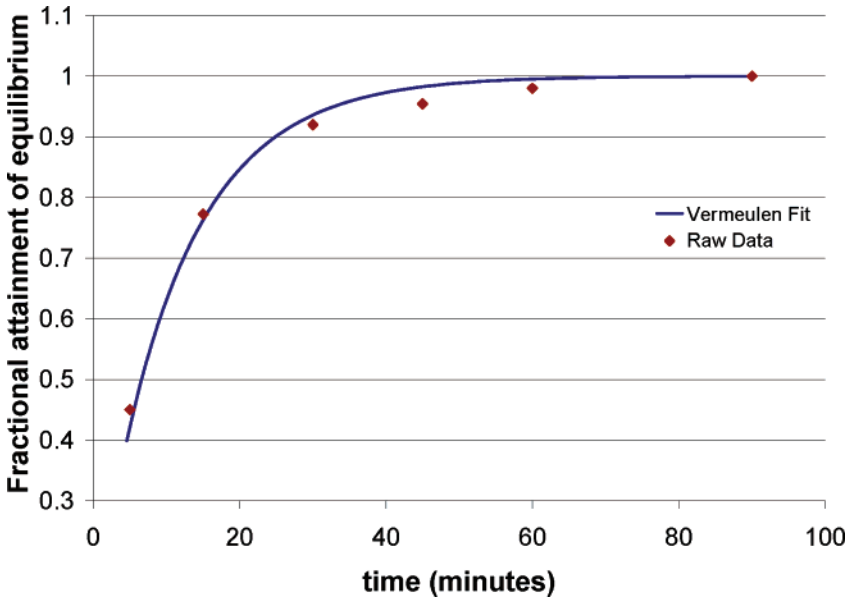

Figure 5. Uptake of ^{90}Sr in $H_{1.45}K_{0.55}ZrSi_3O_9 \cdot 2H_2O$ at neutral pH expressed as the fractional attainment of equilibrium over time.

TGA. Thermogravimetric analysis of compound **1** showed a total weight loss of 13.3% at 850 °C (see Figure 6). The weight loss before 50 °C (1.7%) was attributed to surface water. The residue collected after performing TGA was shown to be amorphous. It was then assumed that the final product had the following composition: $K_{0.56}O_{0.28}/ZrO_2/3SiO_2$. The calculated total weight loss of interstitial water (9.5%) plus the splitting off of water from protons and silicate oxygens (3.4%) summed to 12.9%.

Discussion

Previously, Clearfield and co-workers have synthesized and characterized the behavior of $K_2TiSi_3O_9 \cdot H_2O$ and its protonated phases.[18] The conversion from a noncentrosymmetric orthorhombic space group to a monoclinic phase containing a crystallographic inversion center was observed upon conversion of the parent compound to the acid phase. In the zirconium system, the same transformation occurs. The phase change is not unusual and has been documented. Rocha and co-workers

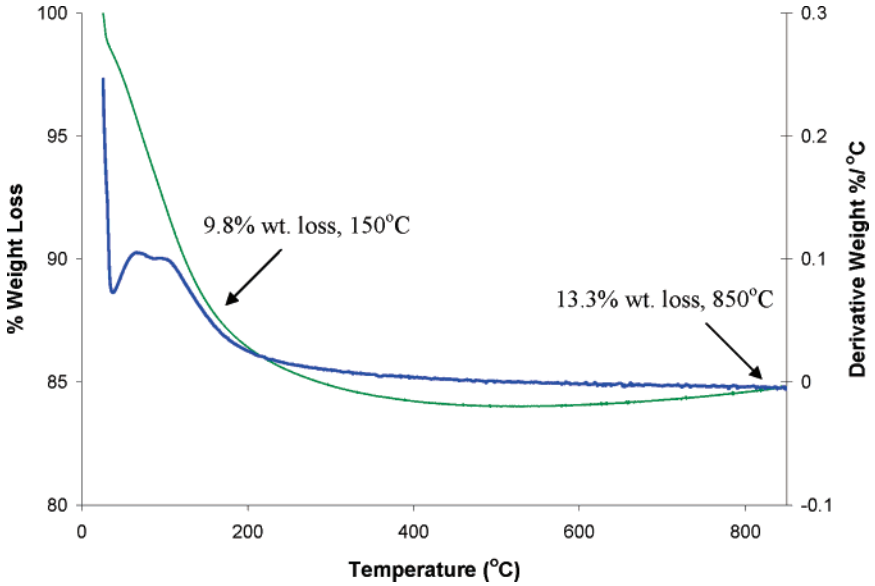

Figure 6. Thermal gravimetric curves of compound **1**. The green line represents the % weight loss as a function of temperature. The blue line is the differential weight loss. Taking into account 1.7% weight loss due to surface water, an internal water loss of 9.8% was noticed, which accounts for 2 mol of water per mole of ion exchanger found in structural refinement.

have hydrothermally synthesized $Na_{0.2}K_{1.8}ZrSi_3O_9 \cdot H_2O$, which crystallizes in the space group $P2_1/c$.[34] In 2001, Rocha and co-workers also synthesized a sodium tin trisilicate, AV-10, crystallizing in the space group $C222_1$.[35]

Liu and Thomas have also reported the titanium analogue of the mixed sodium potassium trisilicate, UND-1, which crystallizes in the space group $P2_1/c$ and was assigned the formula $Na_{2.7}K_{5.3}Ti_4Si_{12}O_{36} \cdot 4H_2O$.[24] In addition to the phase change, other structural similarities exist between the titanium- and zirconium-protonated phases. Both phases maintain the same ion-exchange cavity structure upon conversion to the acid phase. The monoclinic angle is only slightly larger than 90° in both phases (91.181(1)° in the zirconium phase and 91.447(1)° in the titanium phase). Although the framework building blocks of UND-1, AV-7, and AV-10 are different, their pore structures are closely related, and the ion-exchange sites are almost identical. The monoclinic angle in the ion-exchange phases is much smaller than the angles reported by Rocha and Liu in their above-mentioned work. The space group of UND-1 and Rocha's AV-7 are the same, $P2_1/c$, and their beta angles are 104.366(9) and 105.0401(8)°, respectively.[36] The change in space group upon conversion is unclear, but it is not due to any extreme changes in framework linkage that may convert it to an umbite polymorph such as kostylevite. Unpublished data from in situ X-ray diffraction studies point to small shifts in silicon positions and disorder in the cation positions as the cause of the phase change. These shifts destroy the center of symmetry in the $P2_1/c$ space group and must ultimately change the beta angle to 90° once more, reinstituting the orthorhombic phase.

Examination of the pure potassium titanium phase suggested a center of inversion in the orthorhombic cell at 0.25, 0, 0.007. Thus, a small change in atomic positions in the orthorhombic parent compound can generate a center of symmetry, creating a monoclinic space group. For the potassium zirconium phase, the suggested center of symmetry for the titanium phase fits well and duplicates many atoms in the framework, translating them from x, y, z to $-x, -y, -z$. This center of symmetry resides in the middle of site 1 when viewed from the c axis, and neither the cations nor the waters in site 2 fit to the inversion center as they do not have a mirror image.

TABLE 7: Selected Bond Angles (°) for Compound 1 and $K_2ZrSi_3O_9 \cdot H_2O$

bond angle	$K_2ZrSi_3O_9 \cdot H_2O$	$K_{0.56}H_{1.44}ZrSi_3O_9 \cdot 2H_2O$
Zr−O9−Si2	134.63	133.66
Zr−O6−Si2	133.96	133.16
Zr−O7−Si3	149.79	138.84
Zr−O5−Si3	124.12	125.61
Zr−O8−Si4	135.97	135.89
Zr−O10−Si	137.92	138.05
Si2−O11−Si4	134.64	128.25
Si2−O13−Si3	132.48	126.12
Si3−O12−Si4	130.39	125.75

The special positions given for the space group $P2_1/c$ in the international tables of crystallography were transformed into positions in $P2_12_12_1$ by using the transformation matrix in eq 1. This did not reproduce the inversion center described by Bortun et al. but does fit, although poorly, an inversion center to the waters and cations in site 2. Because no inversion center can be fit to the cations in site 2 in the orthorhombic space group that satisfies a point of pseudosymmetry for all atoms in the unit cell, the movement of cations to or from the exchange site likely has no influence on the change in crystal system. The position and occupancy of cations in site 1 are what determines the space group. The change in framework parameters such as bond lengths and bond angles is subtle and not likely to be entirely responsible for the drop in symmetry. Selected bond angles for compound **1** and $K_2ZrSi_3O_9 \cdot H_2O$ are shown in Table 7.

There are, however, differences between the titanium acid phase and the zirconium acid phase trisilicates. There are 2 molecules of water in the protonated zirconium trisilicate, rather than the 1.8 found in the previously studied titanium analogue of similar substitution.[20] In the zirconium phase, these waters are located entirely in site 2, with the remaining potassium found in site 1. This is in contrast to the titanium phase which maintains some potassium in site 1. The disparity demonstrates how the smaller unit cell and therefore the smaller ion-exchange cavities in the titanium phase hold the potassium more tightly. The unit cell volumes respond oppositely upon conversion to the acid phase. The cell volume increases by ~20 Å^3 in the titanium phase, while the corresponding change in the zirconium

phase is a decrease of almost 40 Å^3. Both changes demonstrate the flexibility of the breathable framework and its desire to accommodate a smaller or larger guest cation. Further exemplifying this flexibility is the increase in cell volume; upon 75% incorporation of Cs^+ into $K_2ZrSi_3O_9 \cdot H_2O$, the cell volume increases by approximately 70 Å.[3]

The selectivity series among alkaline earth metals in acidic to neutral pH was shown to be $Ba^{2+} > Sr^{2+} > Ca^{2+} > Mg^{2+}$. According to Eisenman, this type I selectivity behavior is indicative of a system in which the anionic sites are of low field strength.[37] This is true of the trisilicate system, where each framework oxygen may be considered to hold a 2/9 e^- charge. For alkali cations, the selectivity of an ion exchanger for two cations in solution depends only on the differences between their free energy of hydration and the energy of binding to the exchange site. The Gibbs free energy of hydration for alkaline earth cations from Ba^{2+} to Mg^{2+} is -1250, -1380, -1505, and -1830 kJ$\cdot$mol^{-1}.[38] The energy of binding the cation in the exchange site is unknown. For the titanium trisilicate system, Bortun et al. concluded that the free energy of hydration was too large of a barrier to overcome and was not compensated for by the free-energy change when the cation came to rest in the exchange site.[20] Because the pores are larger in **1** than those in the protonic titanium trisilicate, a more favorable free energy of binding inside of the exchanger is possible.

The rates of exchange do not correlate precisely with the selectivity data. Though Ba^{2+} is the most favored cation, the Sr^{2+} cation shows the highest diffusion coefficient. It is important to note that the rates of exchange are defined as mass diffusion, meaning they express the diffusion of all three species involved in the exchange, H^+, K^+, and M^{2+}.

The affinity of the titanium phase for alkaline earth cations is poor, and almost no difference in uptake is observed for Ca^{2+}, Sr^{2+}, and Ba^{2+}; there is only a slight improvement in the equilibrium uptake of group II cations for the zirconium phase. Size discrimination should be the deciding difference in the ability to selectively exchange cations, but an important change arises when moving from group I to group II cations. The enthalpy of hydration for 2+ cations is at least four times greater than that of a 1+ cation. The change in entropy is, however, in the reaction's favor when exchanging a 1+ cation for a 2+.

From a strictly thermodynamic view, it is obvious that the energy of the product must be lower than the energy of the starting material; however, the calculation of a Gibbs energy is not so straightforward concerning ion-exchange reactions, especially if a phase change occurs. ΔG can also be an integral value dependent on the level of exchange over time. In their work with alpha zirconium phosphate, Clearfield and co-workers also demonstrated that the thermodynamics of exchange were correlated with the extent of hydration.[39] It has been shown however that the entropy term dominates in the Gibbs free energy equation for a variety of ion-exchange reactions but is dependent on such factors as the outgoing cation.[40−43] The family of trisilicates would likely show the same trends in entropic driving force, but the question of whether the kinetic data will correlate strongly with thermodynamic data is still unknown.

Conclusion

A partially protonated phase of zirconium trisilicate has been synthesized by ion exchange, and the incorporation of alkaline earth cations has been studied using this new material. Compound **1** is structurally similar to the titanium acid phase and shows the same phase transformation from an orthorhombic to a monoclinic crystal system as that of the previously studied titanium trisilicate upon conversion to the acid phase.

Two strontium ion-exchange phases were derived from the acid phase. Compound **2** is a partially substituted phase in which the strontium cations show no preference for exchange site 1 or site 2. The completely strontium-substituted compound **3** shows slight preference for strontium in exchange site 2. Compounds **2** and **3** maintain the monoclinic space group of the parent compound.

The selectivity of **1** for alkaline earth cations follows the order $Ba^{2+} > Sr^{2+} > Ca^{2+} > Mg^{2+}$. The kinetics of exchange do not mimic this pattern as strontium shows the fastest mass diffusion coefficient.

Work involving the incorporation of lanthanides and use of thorium as a surrogate for plutonium uptake studies are under way.

Acknowledgment. We acknowledge with thanks the U.S. Department of Energy, Environmental Management Science Program Grant No. De-FG07-01ER6300 with funds supplied through Westinghouse Savannah River Technology Center.

References and Notes

(1) Schultz, W. W.; Lombardo, N. J. *Separation Science and Technology for Disposal of Radioactive Tank Waste*; Plenum Press: New York, 1998.

(2) Celestian, A. J.; Mevedev, D. G.; Tripathi, A.; Parise, J. B.; Clearfield, A. *Nucl. Instrum. Methods Phys. Res., Sect. B* **2005**, *61*, 238.

(3) Riddle, S. C. L.; Baker, J. D.; Law, J. D.; McGrath, C. A.; Meikrantz, D. H.; Mincher, B. J.; Peterman, D. R.; Todd, T. A. *Solvent Extr. Ion Exch.* **2005**, *23*, 449.

(4) Liu, C.; Lambert, J. B.; Fub, L. *J. Mater. Chem.* **2004**, *14*, 1303.

(5) Howden, M.; Pilot, J. *Ion Exchange Technology*; Ellis Horwood: Chichester, U.K., 1984; p 66.

(6) Erdem, E.; Karapinar, N.; Donat, R. *J. Colloid Interface Sci.* **2004**, *280*, 309.

(7) Shimizu, K.; Hasegawa, K.; Nakamuro, Y.; Kodamab, T.; Komarnenic, S. *J. Mater. Chem.* **2004**, *14*, 1031.

(8) Griffith, C. S.; Luca, V.; Yee, P.; Sebesta, F. *Sep. Sci. Technol.* **2005**, *40*, 1781.

(9) Aly, H. F.; El-Naggar, I. M. *J. Radioanal. Nucl. Chem.* **1998**, *228*, 151.

(10) El-Naggar, I. M.; El-Absy, M. A.; Aly, H. F. *Colloids Surf.* **1992**, *66*, 28l.

(11) Belinskaya, F. A.; Milizyna, E. A. *Usp. Khim.* **1980**, *49*, 1904.

(12) Abe, M. *Ion Exchange and Solvent Extraction*; Marcel Dekker: New York, 1995.

(13) Clearfield, A. *Solid State Sci.* **2001**, *3*, 103.

(14) Anthony, R. G.; Phillips, C. V.; Dosch, R. G. *Waste Manage.* **1993**, *13*, 503.

(15) Luca, V.; Hanna, J. V.; Smith, M. E.; James, M.; Mitchell, D. R. *Microporous Mater.* **2002**, *55*, 1.

(16) Tripathi, A.; Medvedev, D.; Nyman, M.; Clearfield, A. *J. Solid State Chem.* **2002**, *72*, 175.

(17) Henshaw, D. E. *Mineral. Mag.* **1955**, *30*, 585.

(18) Clearfield, A.; Bortun, A. I.; Bortun, L. N.; Poojary, D. M.; Khainakov, S. A. *J. Mol. Struct.* **1998**, *470*, 207.

(19) Lin, Z.; Rocha, J.; Valente, A. *Chem. Commun.* **1999**, 2489.

(20) Bortun, A. I.; Bortun, L. N.; Poojary, D. M.; Xiang, O.; Clearfield, A. *Chem. Mater.* **2000**, *12*, 294.

(21) Pertierra, P.; Salvadó, M. A.; Garcia-Granda, S.; Khainakov, S. A.; Garcia, J. R. *Thermochim. Acta* **2004**, *423*, 113.

(22) Plevert, J.; Sanchez-Smith, R.; Gentz, T. M.; Li, H.; Groy, T. L.; Yaghi, O. M.; O' Keeffe, M. *Inorg. Chem.* **2003**, *42*, 5954.

(23) Liu, X.; Shang, M.; Thomas, J. K. *Microporous Mater.* **1997**, *10*, 273.

(24) Poojary, D. M.; Bortun, A. I.; Bortun, L. N.; Clearfield, A. *Inorg. Chem.* **1997**, *36*, 3072.

(25) Fewox, C. S.; Kirumakki, S.; Clearfield, A. *Chem. Mater.* **2007**, *19*, 384.

(26) Rodriguez-Carvajal, J. *Abstracts of the Satellite Meeting on Powder Diffraction of the XV Congress of the IUCr*; Toulouse, France 1990; p 127.

(27) Roisnel, T.; J. Rodríguez-Carvajal, J. *Science Forum*, Proceedings of the Seventh European Powder Diffraction Conference (EPDIC 7); 2000; p 118.

(28) Rodríguez-Carvajal, J.; Roisnel, T. *Commission for Powder Diffraction, International Union for Crystallography Newletter (May-August) Summer*; 1998.

(29) Larson, A.; Dreele, R. B. *GSAS: Generalized Structure Analysis System*, LANSCE, Los Alamos National Laboratory, Los Alamos, NM; Reagents of the University of California, CA, 1985−1988.

(30) Le Bail, A.; Duroy, H.; Fourquet, J. L. *Mater. Res. Bull*. **1988**, *23*, 4467.

(31) Helfferich, F. *Ion Exchange*; McGraw-Hill: New York, 1962.

(32) Zou, X.; Dadachov, M. S. *Acta Crystallogr., Sect. C* **2000**, *56*, 738.

(33) Shannon, R. D.; Prewitt, C. T. *Acta Crystallogr., Sect. B* **1969**, *25*, 925.

(34) Ferreira, P.; Ferreira, A.; Rocha, J.; Soares, M. R. *Chem. Mater.* **2001**, *13*, 355.

(35) Ferreira, A.; Lin, Z.; Rocha, J.; Morais, C. M.; Lopes, M.; Fernandez, C. *Inorg. Chem.* **2001**, *40*, 3330.

(36) Lin, Z.; Rocha, J.; Pedrosa de Jesusa, J. D.; Ferreirab, A. *J. Mater. Chem.* **2000**, *10*, 1353.

(37) Eisenman, G. *Biophys. J.* **1962**, *2*, 259.

(38) Marcus, Y. *J. Chem. Soc., Faraday Trans.* **1991**, *87*, 2995.

(39) Kullberg, L.; Clearfield, A. *J. Phys. Chem.* **1981**, *85*, 1585.

(40) Roca, S.; Airoldi, C. *Thermochim. Acta* **1996**, *1*, 289.

(41) Chen, S.; Chao, K.; Leet, T. *Ind. Eng. Chem. Res.* **1990**, *29*, 2020.

(42) Keane, M. A. *Microporous Mater.* **1995**, *3*, 394.

(43) Tarasevich, Y. I.; Krysenko, D. A.; Polyakov, V. E. *Theor. Exp. Chem.* **2006**, *42*, 320.